Photocarrier lifetime and transport in silicon supersaturated with sulfur

Peter D. Persans,[1] Nathaniel E. Berry,[1,a)] Daniel Recht,[2] David Hutchinson,[1] Hannah Peterson,[1,3,b)] Jessica Clark,[1,c)] Supakit Charnvanichborikarn,[4,d)] James S. Williams,[2,4] Anthony DiFranzo,[1,e)] Michael J. Aziz,[2] and Jeffrey M. Warrender[3]
[1]*Rensselaer Polytechnic Institute, 110 8th Street, Troy, New York 12180, USA*
[2]*Harvard School of Engineering and Applied Sciences, Cambridge, Massachusetts 02138, USA*
[3]*US Army – ARDEC, Benet Laboratories, Watervliet, New York 12189, USA*
[4]*Research School of Physics and Engineering, ANU, Canberra 0200, Australia*

(Received 18 April 2012; accepted 1 August 2012; published online 11 September 2012)

Doping of silicon-on-insulator layers with sulfur to concentrations far above equilibrium by ion implantation and pulsed laser melting can result in large concentration gradients. Photocarriers generated in and near the impurity gradient can separate into different coplanar transport layers, leading to enhanced photocarrier lifetimes in thin silicon-on-insulator films. The depth from which holes escape the heavily doped region places a lower limit on the minority carrier mobility-lifetime product of 10^{-8} cm^2/V for heavily sulfur doped silicon. We conclude that the cross-section for recombination through S impurities at this concentration is significantly reduced relative to isolated impurities. © *2012 American Institute of Physics*. [http://dx.doi.org/10.1063/1.4746752]

It has been proposed that the introduction of a narrow band of delocalized impurity states deep in the gap of a semiconductor can lead to sub-gap absorption without the concomitant large decrease in carrier lifetime due to non-radiative recombination[1–3] through localized recombination centers. Indirect evidence for such lifetime enhancement in heavily Ti-doped Si has been recently reported.[4] Another important candidate system is the chalcogen (S, Se, Te) impurity in silicon, for which an insulator-metal transition has recently been reported[5,6] Photodiodes incorporating chalcogen-hyperdoped layers exhibit high photocarrier gain and enhanced response in the near infrared.[7,8] Although the properties of dilute sulfur impurities in silicon are well known, the optoelectronic properties of heavily chalcogen doped silicon are not well studied. In the current work, we use the wavelength dependence of photocurrent response to deduce the mobility-lifetime product of photoexcited minority carriers (holes) in silicon hyperdoped with sulfur.

Although the energy of the isolated S donor state is $\sim$318 meV below the conduction band edge,[9] the nature and depth of the impurity states for heavily doped material are the subject of active research.[5,6,10] The nature of the impurity states can have a profound effect on the mobility lifetime product. The range of expected mobility-lifetime products can be estimated from two extreme assumptions. At one extreme, Shockley-Read-Hall recombination is negligible so the hole lifetime is limited by Auger recombination and, for a free electron density of 10^{19} cm^{-3}, the lifetime is of order 10^{-8} s.[11] At the other extreme, assuming that the lifetime is entirely controlled by Shockley-Read-Hall recombination through 10^{19} cm^{-3} neutral localized impurity states near midgap, the lifetime is expected to be of order 10^{-12} s (Refs. 12 and 13). Assuming a widest plausible range of photocarrier mobility of 30 to 100 cm^2/Vs, consistent with Hall measurements on similar material[14,15] and extrapolation of drift mobility in heavily doped material,[16] the potential range for mobility-lifetime product can be from 3×10^{-11} to 10^{-6} cm^2/V, depending on whether Shockley-Read-Hall recombination is reduced in heavily doped material.

In order to achieve the high active dopant density necessary for impurity band delocalization, a materials processing approach involving ion implantation followed by pulsed laser melting and rapid solidification has been employed.[15,17] Optically smooth crystalline silicon, supersaturated with nearly one atomic percent sulfur, has been fabricated by this approach.[15,17,18] Implantation and pulsed laser melting leads to a shallow n+/substrate junction with a large concentration gradient.[15,19] This concentration gradient produces a large electric field that separates different types of carriers created near the junction.

Following the procedure of Pan *et al*.[20] Si:S layers were formed in the device layer of silicon on insulator (SOI) wafers (p-type, B-doped, 13.5–22.5 Ωcm) with a 260 nm Si device layer atop a 1 μm buried oxide on a thick Si substrate. The 260 nm Si layer was ion implanted at room temperature with 70 keV Si+ to a dose of 3×10^{15} ions/cm^2 for preamorphization, followed by 80 keV ^{32}S+ to a dose of 1×10^{15} ions/cm^2. All implantation energies were chosen to yield an average ion projected range of $\sim$80 nm. Under these conditions, the implantation dose was sufficient to amorphize roughly the top 200 nm of the 260 nm device layer. The samples were subsequently irradiated with one pulse from a spatially homogenized, pulsed XeCl+ excimer laser (308 nm, 25 ns full width at half maximum, 50 ns pulse duration, 0.6–0.7 J/cm^2) with a square spot approximately 3×3 mm^2. The laser fluence was chosen to melt the entire damaged region while preserving the deepest few nm of crystalline seed for epitaxial single-crystal growth.[18] These silicon-on-insulator

a)Present address: University of Pennsylvania, Philadelphia, Pennsylvania 19104-6391, USA.
b)Present address: University of Washington, Seattle, Washington 98195, USA.
c)Present address: University of Maine, Orono, Maine 04469, USA.
d)Present address: Lawrence Livermore National Laboratory, Livermore, California 94550, USA.
e)Present address: University of California at Irvine, Irvine, California 92697, USA.

 © 2012 American Institute of Physics

structures, heavily doped by implantation and laser melting, have two key doping regions: the heavily doped top 200 nm and the thin unmelted B-doped seed region.

Ohmic gold surface contacts for coplanar photocurrent measurements were evaporated with a 0.8 mm gap. The sample resistance at room temperature is $\sim 1500\,\Omega$. Coplanar photocurrent is small compared with dark current, so chopped light and lock-in techniques are required. Photocurrent is normalized by the incident photon flux to produce external quantum efficiency. Light from a selection of light emitting diodes was passed through a 10 nm bandpass monochromator to provide well defined excitation energies.

We have previously shown[21] that coplanar photocurrent in sulfur-hyperdoped silicon-on-insulator structures is limited by extraction or recombination of holes that transit the sample in the less-highly doped seed layer as shown schematically in Fig. 1. Both electrons and holes contribute to observed photocurrent, but saturation of photocurrent with increased bias voltage is attributed to hole extraction. The external quantum collection efficiency, therefore, depends on the depth at which a hole is generated, the probability that the hole can transfer to the seed layer, and the probability that the hole drifts to the contact in the seed layer. The transfer of photogenerated carriers to or from hyperdoped to seed layers depends on the details of the local fields. The depth at which photocarriers are created can be varied by varying the excitation wavelength, therefore analysis of the external photocurrent collection efficiency can be used to deduce the transport properties of holes in the hyperdoped layer.

The potential profile and field can be computed by integration of Poisson's equation including ionized dopants and free electron density. Because the donor energy is not known, there is uncertainty in the computed profile, but an order of magnitude estimate can be made. The sulfur doping profile measured using secondary-ion mass spectrometry for a sulfur implantation dose of $10^{15}\,\mathrm{cm}^{-2}$, followed by pulsed laser melting, is shown in Figure 2. The free carrier density is about 10% of the sulfur density at room temperature. There is a broad peak in sulfur concentration of about 2.5×10^{19} atoms/cm^3 at a depth x of about 110 nm, with a sharp fall off between $x = 130$ and 250 nm. It is likely that the sharp increase in sulfur concentration near the surface is part of a surface oxide layer and is, therefore, neglected here in the calculation of the potential profile. The resulting potential profile for holes, found by integrating Poisson's equation assuming that the donor density is equal to the sulfur density, is shown in Figure 3. Depending on assumptions for the depth and activity of impurities, a confining well of

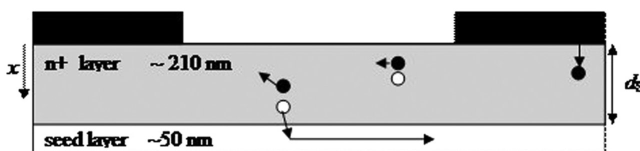

FIG. 1. A model for photoexcitation and co-planar transport in a silicon-on-insulator hyperdoped Si/seed multilayer stack. Absorption of a photon with energy greater than the gap produces an electron hole pair. If the hole can escape the hyperdoped region, then it can traverse the sample in the seed layer. If the hole remains in the hyperdoped layer, then the lifetime is expected to be very short.

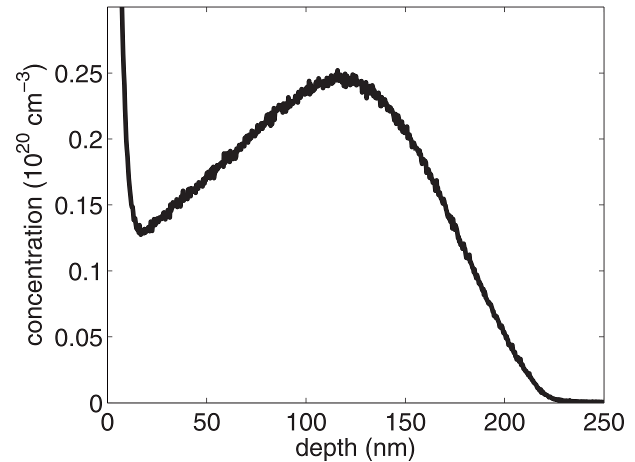

FIG. 2. Sulfur concentration after implantation and laser melting determined by SIMS plotted against depth. The large increase near the surface is likely due to a surface oxide.

depth 0.1 to 0.2 eV for holes is computationally found near the bottom oxide interface. The presence of the hole well at the back surface is independent of assumptions about front surface sulfur. The electric field is 1000 V/cm at $x = 140$ nm and increases to 7000 V/cm at $x = 250$ nm. The computed field strength and potential well depth is sufficient to separate electrons and holes and to confine holes to the seed layer once the holes transfer into it. We note that a similar carrier separation mechanism has been suggested to explain lifetime enhancement in proton implanted p-type silicon.[22]

The mobility-lifetime product for holes in the seed layer is of order $\mu_S \tau_S = 3 \times 10^{-3}\,\mathrm{cm}^2/\mathrm{V}$ (Ref. 21) which is more than three orders of magnitude greater than the highest mobility-lifetime product estimated above for hyperdoped material. The effective photocarrier lifetime, from the time-resolved photocurrent transient, extrapolated to zero external source-drain field, is 40 μs. The hole photocurrent is therefore likely to be dominated by holes generated in or transferred to the seed layer. With this assumption, the hole contribution to coplanar photocurrent Δi is given by the product of the net rate R at which holes are generated in or

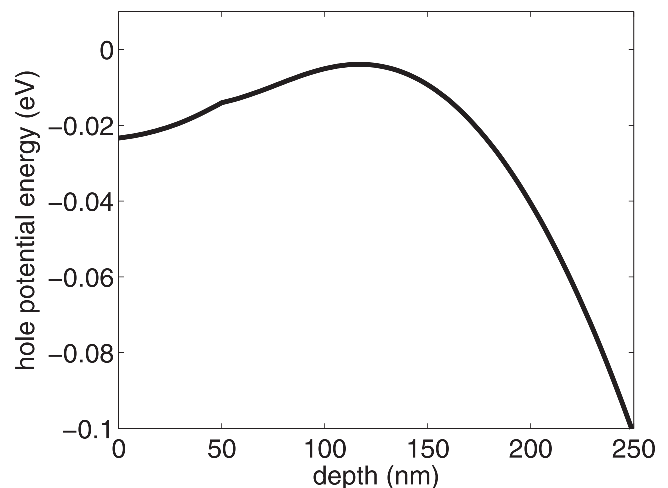

FIG. 3. Potential energy for holes, computed by integration of Poisson's equation assuming a donor level 100 meV below the conduction band edge, plotted as a function of depth. The sulfur buildup in the first 10 nm is neglected for this calculation.

enter the seed layer and the probability of extraction of a hole once it enters the seed layer. If holes are uniformly transferred into the seed layer and drift under action of the field to the contact, the probability of extraction approaches unity for a moderate lateral field of >20 V/cm in a sample with a 1 mm gap. The photocurrent is thus given by $\Delta i_p = eR = e\int r(x)dx$. The rate $r(x)$ at which holes generated at a given depth transfer to the seed layer is given by the product of the depth-dependent generation rate $G(x)$ and the depth-dependent probability density of escape to the seed layer $P(x)$ so that $R = \int G(x)P(x)dx$.

Holes created at depth x drift and diffuse between hyperdoped and seed layers under the action of a large field E. A full calculation of the depth dependent probability of transfer to the seed layer involves estimates of the local lifetime, which requires assumptions about the recombination mechanisms. In order to deduce an approximate mobility-lifetime product, a single effective average mobility-lifetime product is assumed for the hyperdoped layer. Using a simple drift approximation, the probability $P(x)$ of escape to the seed layer under action of the field is given by $P(x)dx = \begin{cases} dx & \text{for } L_D < (d_S - x) \\ 0 & \text{for } L_D > (d_S - x) \end{cases}$, where the effective interface between seed and hyperdoped layers is at depth d_S and the diffusion length, L_D, is the lesser of $e\mu_h\tau_h E$ and D where D is the thickness of the high field region and $\mu_h\tau_h$ is the mobility-lifetime product for holes in the hyperdoped layer. (For holes generated in the seed layer, $P = 1$.)

As an example optical calculation, in Figure 4, we divide the sample into five SOI sub-layers. The choice of five layers in this example is intended to display the overall behavior as simply as possible. Full calculations involved many more layers. The optical absorptance in each layer is computed, including multiple reflections and interference from the oxide and top interfaces, as described elsewhere.[23,24]

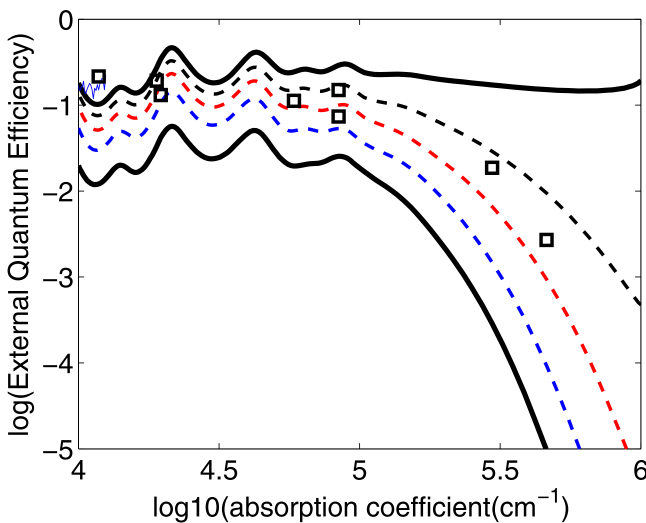

FIG. 4. Measured external quantum efficiency and simulated absorption in layers of the doped SOI sample. The squares are the quantum efficiency measured at individual wavelengths using lasers and light emitting diodes. The lowest solid curve (a) is the absorption in the bottom 50 nm of the silicon. The next curve (b) is the absorption in the bottom 100 nm. Curve (c) is the absorption in the bottom 150 nm. Curve (d) is the absorption in the bottom 200 nm. The uppermost solid curve (e) is the total absorption.

The bottom 50 nm is assumed to be pure silicon. For the top 210 nm, we use the optical constants for hyperdoped silicon from Pan *et al.*[20] The spectrum of the accumulated absorption in layers starting at the back surface and adding 50 nm increments is shown in Figure 4. If only carriers generated in the seed layer contribute to photocurrent, then curve (a) is expected. If carriers generated everywhere except the top 60 nm contribute, then curve (d) is expected.

The measured external quantum efficiency is plotted in Figure 4 as individual points. External quantum efficiency from 2.5 to 3 eV is only weakly dependent on energy. The quantum efficiency at 3.30 eV is 3×10^{-2}, consistent with contribution from a total thickness of 170 ± 20 nm, therefore holes are collected from the entire region in which the field pulls holes to the seed layer. Since holes are able to drift or diffuse across ~100 nm of hyperdoped silicon with a field of ~1000 V/cm, it is possible to place a lower limit on the mobility lifetime product for holes in hyperdoped material of 10^{-8} cm^2/V.

For every hole separated into the seed layer, there is a corresponding electron in the hyperdoped layer which could undergo photoconductive gain. The absence of photoconductive gain implies that the electron drift mobility is less than 160 cm^2/Vs, consistent with Hall measurements on similar material.[14] The absence of photocurrent response in the infrared, as previously reported,[21] sets an upper limit for the electron mobility-lifetime product of 10^{-7} cm^2/V.

The mobility-lifetime product found here for a doping level of $\sim 2 \times 10^{19}$ cm^{-3} is over 100 times greater than that predicted for Shockley-Read-Hall recombination through isolated neutral impurities. We conclude that the cross-section for recombination through S impurities at this concentration is significantly reduced relative to isolated impurities. This reduction could be due to formation of an impurity band as proposed by Luque and Marti[2,3] or due to broadening of the impurity band at high density toward the conduction band edge.[6] Clustering of sulfur atoms is unlikely to be responsible for the reduced rate of Shockley-Read-Hall recombination since 100-atom clusters would have been visible in previous cross-section transmission electron microscopy studies.[15] It is unlikely that the impurity band has broadened into the conduction band because the insulator to metal transition occurs at a sulfur concentration of about 3×10^{20} cm^{-3},[5] somewhat higher than the concentration in this study. Further studies with varying doping levels may elucidate the mechanisms for lifetime enhancement.

Research at Rensselaer was supported by the Army Research Office under Contract No. W911NF0910470 and by the NSF REU program at Rensselaer. Research at Harvard was supported by US Army ARDEC under Contract No. W15QKN-07-P-0092. D.R. was supported in part by a National Defense Science and Engineering Graduate fellowship. We thank Athena Pan and Mark Winkler for access to unpublished data. We thank William Cunningham, David Lombardo, Andrew McAllister, Christina McGahan, Jeremy Mehta, and Drew Rosen for technical assistance.

[1] A. Luque and A. Marti, Phys. Rev. Lett. **78**(26), 5014 (1997).
[2] A. Luque, A. Marti, E. Antolin, and C. Tablero, Physica B **382**(1–2), 320 (2006).

[3]A. Marti, L. Cuadra, N. Lopez, and A. Luque, Semiconductors **38**(8), 946 (2004).
[4]E. Antolin, A. Marti, J. Olea, D. Pastor, G. Gonzalez-Diaz, I. Martil, and A. Luque, Appl. Phys. Lett. **94**(4), 042115 (2009).
[5]M. Winkler, D. Recht, M.-J. Sher, A. J. Said, E. Mazur, and M. J. Aziz, Phys. Rev. Lett. **106**, 178701 (2011).
[6]E. Ertekin, M. T. Winkler, D. Recht, A. J. Said, M. J. Aziz, T. Buonassisi, and J. C. Grossman, Phys. Rev. Lett. **108**(2), 026401 (2012).
[7]J. E. Carey, C. H. Crouch, M. Y. Shen, and E. Mazur, Opt. Lett. **30**(14), 1773 (2005).
[8]A. J. Said, D. Recht, J. T. Sullivan, J. M. Warrender, T. Buonassisi, P. D. Persans, and M. J. Aziz, Appl. Phys. Lett. **99**, 073503 (2011).
[9]H. G. Grimmeiss and E. Janzen, in *Handbook on Semiconductors*, edited by T. S. Moss and S. Mahajan (Elsevier, Amsterdam, 1994), Vol. 3, p. 1755.
[10]M. Winkler and E. Mazur, in *2008 Conference on Lasers and Electro-Optics & Quantum Electronics and Laser Science Conference* (2008), Vols. 1–9, pp. 1053.
[11]J. Dziewior and W. Schmid, Appl. Phys. Lett. **31**(5), 346 (1977).
[12]R. H. Bube, *Photoconductivity of Solids*. (Krieger, New York, 1978).
[13]J. M. Fairfield and B. V. Gokhale, Solid-State Electron. **8**(8), 685 (1965).
[14]M. Winkler, Ph.D. dissertation, Harvard, 2010, p. 117.
[15]M. Tabbal, T. G. Kim, J. M. Warrender, M. J. Aziz, B. L. Cardozo, and R. S. Goldman, J. Vac. Sci. Technol. B **25**, 1847 (2007).
[16]S. M. Sze, *Physics of Semiconductor Devices* (Wiley, New York, 1981), p. 29.
[17]B. P. Bob, A. Kohno, S. Charnvanichborikarn, J. M. Warrender, I. Umezu, M. Tabbal, J. S. Williams, and M. J. Aziz, J. Appl. Phys. **107**(12), 123506 (2010).
[18]T. G. Kim, J. M. Warrender, and M. J. Aziz, Appl. Phys. Lett. **88**, 241902 (2006).
[19]D. Recht, J. T. Sullivan, R. Reedy, T. Buonassisi, and M. J. Aziz, Appl. Phys. Lett. **100**, 112112 (2012).
[20]S. H. Pan, D. Recht, S. Charnvanichborikarn, J. S. Williams, and M. J. Aziz, Appl. Phys. Lett. **98**, 121913 (2011).
[21]P. D. Persans, N. E. Berry, D. Recht, D. Hutchinson, A. Said, J. M. Warrender, H. Peterson, A. DiFranzo, C. McGahan, J. Clark, W. Cunningham, and M. J. Aziz, in Mater. Res. Soc. Conf. Proc. (2011), Vol. 1321, p. mrss11.
[22]D. C. Leung, P. R. Nelson, O. M. Stafsudd, J. B. Parkinson, and G. E. Davis, Appl. Phys. Lett. **67**, 88 (1995).
[23]V. Vuitton, B. N. Tran, P. D. Persans, and J. P. Ferris, Icarus **203**, 663 (2009).
[24]See supplementary material at http://dx.doi.org/10.1063/1.4746752 for dark IV curves, photoconductivity response spectra, and band diagrams.